Original Article

Ship hull–propeller system optimization based on the multi-objective evolutionary algorithm

Hassan Ghassemi and Hassan Zakerdoost

Abstract
The optimization of the hull–propeller system of a ship has always been one of the most important aspects of design in order to reduce the costs, mechanical losses and increase the life of system components. The proposed design methodology represents a comprehensive approach to optimize the hull–propeller system simultaneously. In this study, two objective functions are considered, i.e. lifetime fuel consumption (LFC) and lifetime cost function (Cost). The mission profile of the vessel is adopted to minimize the LFC and Cost over their operational life. The well-known evolutionary algorithm based on NSGA-II is employed to handle the multi-objective problems, where the main propeller and hull coefficients are the unknown and are considered as design variables. The results are presented for a commercial container ship driven by B-series propeller. Three different engines with the same mission profile were taken and the results revealed that the proposed method is an appropriate and effective approach for finding Pareto optimal solutions distributed uniformly and is able to improve both of the objective functions significantly and other performances of the system.

Introduction

Optimization problems have many applications in real life. Many real-world and theoretical problems may be modeled in this general framework.[1–3] *A priori* and *a posteriori* are generally two approaches for optimizing multi-objective problems (MOPs). Many problems employed the a priori approach such as scalarization technique, where all preference information about fitness functions and their relative importance is known in advance. In the a posteriori approach such as evolutionary algorithms, preference information is used a posteriori, i.e. the algorithm generates a set of efficient solutions of which the decision maker choose one of them by a decision making skill.[4]

The optimization of ship hull–propeller system is one of the most important aspects of ship design and results in ship cost reduction, improving performance and increasing the lifetime of propulsion system. For a comprehensive and detailed ship hydrodynamic optimization all objective functions influencing problem solving need to be considered, because it is clear that consideration of an objective function without the other ones gives unrealistic and impractical results. In addition to the parameters that usually are considered in propeller design, skew can be used

as another important parameter for propeller optimization. This parameter affects cavitation and propeller efficiency. In the 21st century, there has been a remarkable amount of work in the field of the hull or propeller optimization. When there is an ability to do optimization of the hull–propeller system simultaneously, it would be probably less efficient to accomplish the optimization separately.

A method based on Michell's thin ship theory is presented by Day and Doctors[5] to calculate the wave wake generated by a ship. They used the elemental tent functions as building blocks to represent the hull form of the ship. Dejhalla et al.[6] proposed a genetic algorithm (GA)-based optimization technique for the optimization of a ship hull from a hydrodynamic point of view. In the optimization procedure, wave resistance was selected as an objective function. The GA was coupled with the well-known Dawson panel

Department of Maritime Engineering, Amirkabir University of Technology, Tehran, Iran

Corresponding author:
Hassan Ghassemi, Department of Maritime Engineering, Amirkabir University of Technology, Hafez Avenue, Tehran 15875–4413, Iran.
Email: gasemi@aut.ac.ir

method for solving the potential flow around a ship hull. Zaraphonitis et al.[7] developed a hull form optimization procedure for minimum wash and total resistance of high speed vessels based on the integration of three software packages: a ship design software package (namely NAPA) for the hull form generation, Ship flow to perform the hydrodynamic evaluation of each hull form and the hull form optimization was done by modeFRONTIER. In another study a hull form with respect to seakeeping and total resistance as objective functions was optimized by using evolutionary strategies.[8] Grigoropoulos and Chalkias[9] selected evolutionary strategies for the hull form optimization with respect to its performance in calm and rough water. Kim and Yang[10] presented a hydrodynamic computational tool for evaluating the steady free-surface flow about a catamaran. They used the Neumann–Michell linear flow model to calculate and GA to minimize total resistance. Zakerdoost et al.[11] proposed a numerical method for optimizing hull form in calm water with respect to total drag. The corrected linearized thin-ship theory was employed to estimate wave drag and the evolution strategy which is a member of the evolutionary algorithms family to minimize the total drag of Series 60 hull form by considering some design constraints. A set of computational tools were used by Gaggero and Brizzolara[12] for the preliminary and detailed designs of SWATH ship. Huang et al.[13] applied a new swarm intelligence-based optimization algorithm, called the artificial bee colony (ABC) algorithm to minimize two ship hull forms with respect to resistance. The Neumann–Michell theory was employed to evaluate the wave resistance.

In the field of the ship propeller optimization, Lee and Lin[14] performed a ship propeller optimization to maximize the B-series propeller efficiency by utilizing the GA. A numerical optimization technique was developed by Cho and Lee[15] to determine the optimum propeller blade shape for efficiency improvement. A self-twisting propeller was optimized by Plucinski et al.,[16] using the GA. They considered the orientation angles of the fibers in each layer as the design variables of efficiency improvement for an optimum design. Burger[17] developed a program to analyze propeller performance based on the GA as an efficient optimization algorithm. Chen and Shih[18] designed an optimum propeller by considering the vibration and efficiency as objective functions and cavitation, strength, and power as constraints in the GA-based optimization of the B-series propeller. Kuiper[19] optimized a large container ship propeller to maximize propeller efficiency at a certain desired speed. Gaafary et al.[20] developed a design optimization technique for the B-series marine propellers with a similar objective as previous work at a single speed. A multi-objective propeller optimization program was implemented by Xie[21] to simultaneously maximize the propeller efficiency and thrust coefficient at a single design speed. The well-known NSGA-II was used to approximate the Pareto solutions of B-series propeller optimization. Mirjalili et al.[22] employed multi-objective particle swarm optimization (MOPSO) to maximize the efficiency and minimize the cavitation of marine propellers simultaneously. They utilized the shape and number of blades and operating conditions as design variables. Kamarlouei et al.[23] presented a numerical method to evaluate the hydrodynamic performances including minimum cavitation, highest efficiency and acceptable blade strength. The evolution strategy technique was used as an optimization algorithm and main structural parameters as design variables to optimize the well-known B-series and DTRC propellers at the design speed of typical ships. Readers can refer to other works[24–27] for more study on the propeller optimization.

In the recent years, some research was dedicated to reduce the LFC. Motley et al.[28] considered the propeller, prime mover, and vessel as one integrated system and employed the probabilistic operational profile of the vessel to minimize the LFC. They evaluated the tradeoffs between different design objectives and constraints by considering the system performance characteristics along with the probability of occurrence, and hence allowed for the global optimization of the propeller geometry. Nelson et al.[29] presented an approach to optimize the propeller–hull system simultaneously in order to design a vessel to have minimal LFC. They used a probabilistic mission profile, propeller–hull interaction, and engine information to determine the coupled container ship and B-series propeller system with minimum fuel cost over its operational life. Other techniques such as neural networks and Bayesian networks[30] can be used for ship optimization problem, if the costly solvers such as CFD/BEM was employed in this problem, but this will be our future work.

This paper concentrates on the multi-objective evolutionary optimization of the coupled propeller and hull system of a vessel using the well-known NSGA-II. The ultimate objective is to design a hull–propeller system with the minimum LFC and Cost function. In order to reach these objectives, the propeller and hull system should be designed in such a way that the ship hull resistance will be minimized and the propeller efficiency maximized. A commercial container ship is selected with the same mission profile and three engines with distinct properties. The following sections are planned as follows: the forthcoming section discusses the problem theory and governing mathematical formulation for calculating resistance, propeller characteristics, and fuel consumption. Next, an explanation of the MOP in particular the NSGA-II based optimization is described. The results and discussion of three MOPs based on three different specific fuel oil consumption (SFOC) curves provided by the engine manufacturers Wartsila, MAN, and Caterpillar are then presented. Finally, the last section

concludes the work and suggests some directions for future research.

General problem formulation

Resistance calculation

The total calm water drag of a ship at a given speed is the force required for the ship to move at that speed. The total drag is made up of two components: the viscous drag, due to moving the ship through a viscous fluid and the wave drag, due to moving the ship on the surface of the water. The wave drag resulted from energy dissipation in the formation of waves on the water surface. The total drag coefficient is

$$C_T = C_v + C_w \tag{1}$$

where C_v is the viscous drag coefficient and C_w is the wave drag coefficient. The viscous drag is composed of frictional drag and pressure drag, i.e. $C_v = (1 + k) C_f$ and C_f is the frictional drag coefficient and k is the form factor which is determined by

$$k = 0.6\sqrt{\nabla/L^3} + 9\nabla/L^3, \quad 0.05 \leqslant k \leqslant 0.4 \tag{2}$$

where L and ∇ are the length and displaced volume of the ship. The frictional drag coefficient is calculated by ITTC'57 as follows

$$C_f = \frac{0.075}{(\log_{10} Rn - 2)^2} \tag{3}$$

where Rn is the Reynolds number.

When the body like ship moves in the surface of water the wave generated due to high pressure at the fore and aft part of it called wave-making drag. There are some theories to determine the wave-making drag like Michell's theory. This theory is valid only under certain restrictive conditions that the fluid is homogenous, incompressible, inviscid and hence the flow is irrotational, surface tension effects can be neglected, the slope of the hull surface relative to the centerplane is small (slender hull), the wave heights generated by the ship hull are small compared with their lengths, the ship does not experience any sinkage or trim and that the water is infinitely deep and laterally unbounded. The coordinate system is depicted in Figure 1.

Based on the energy flux far from the ship, the equation for the wave drag is

$$R_w = \frac{\pi}{2}\rho V^2 \int_{-\pi/2}^{\pi/2} \left|A(\theta)\right|^2 \cos^3(\theta)\, \mathrm{d}\theta \tag{4}$$

where V is the ship velocity, ρ is the water density, θ is the angle between the direction of the moving ship and that of a propagating wave and $A(\theta)$ is the amplitude function specific to hull shape, sometimes also
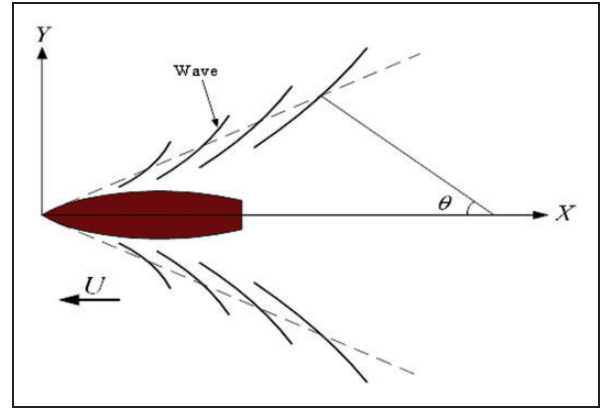

Figure 1. Coordinate system of Michell's thin ship theory.

called the free wave spectrum and describes the far field ship waves. The amplitude function is the only term dependent on hull shape and can be calculated by experimental measurement or by approximation such as small disturbance theory. For a mono-hull based on Michell's thin ship theory the amplitude function is as follows

$$
\begin{aligned}
A(\theta) = {} & \frac{2}{\pi}(k_0 \ \sec^3\theta) \int_{-\infty}^{0}\int_{-\infty}^{\infty} \\
& \times Y_x(x,z)e^{ik_0 x \sec\theta}e^{k_0 z \sec^2\theta}\mathrm{d}x\mathrm{d}z
\end{aligned}
\tag{5}
$$

Working with the hull offsets $Y(x,z)$ is usually preferred over working with the slope of the offsets $Y_x(x,z)$; hence this equation is integrated by parts including only the transom stern

$$
\begin{aligned}
A(\theta) = {} & -\frac{2i}{\pi}(k_0 \sec^2\theta)^2 \int_{-\infty}^{0}\int_{-\infty}^{\infty} \\
& \times Y(x,z)e^{ik_0 x \sec\theta}e^{k_0 z \sec^2\theta}\mathrm{d}x\mathrm{d}z \\
& + \frac{2}{\pi}(k_0 \sec^3\theta) \int_{-\infty}^{0} Y(x_s,z)e^{ik_0 x_s \sec\theta}e^{k_0 z \sec^2\theta}\mathrm{d}z
\end{aligned}
\tag{6}
$$

where $k_0 = \frac{g}{V^2}$, g is the acceleration of gravity, $y = \pm Y(x,z)$ is the equation or offsets of the submerged hull, and $Y(x_s,z)$ indicate the nonzero transom stern offsets. In this equation the offsets of bow is assumed zero, otherwise will be added a complexity to the equation. The wave resistance coefficient follows by normalization according to

$$C_w = \frac{R_w}{0.5\rho S V^2} \tag{7}$$

with R_w and S denoting the wave making resistance and (static) wetted surface area, respectively.

Using Michell's integral for wave making resistance and the ITTC line with a form factor for viscous drag leads to rather good agreement. For the entire range of Froude number, errors between predictions
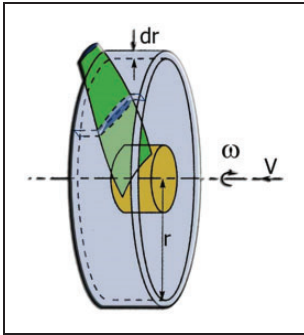
Figure 2. A propeller blade divided into discrete number of sections.

Figure 3. Velocity and force components of a section of propeller blade in BET.

and the experimental curve lie within acceptable value.[10] The current method used for calculating the total resistance is relatively cost effective and less time consuming compared to other complex CFD methods and hence is a suitable technique for the current MOPs.

The integrand of above amplitude function is highly oscillatory, and special techniques are needed to evaluate the integrals. We use Filon's quadrature[31] to capture the rapid oscillations as $|\theta| \to \pi/2$. Conventional quadratures fail to capture the correct decay of the spectrum in this region.[32]

Propeller performance computation

The blade element theory (BET) is one of different methods for calculating propeller performance. The BET in contrast to the momentum theory is concerned with how a propeller generates its thrust and how this thrust depends upon the shape of propeller blades. The propeller blade is divided into the discrete number of sections, each of these elements is then treated like hydrofoil subjected to an incident velocity V_1 and hence produces a hydrodynamic force due to its motion through the fluid. The axial component of this hydrodynamic force is the element thrust while the moment about the propeller axis of the tangential component is the element torque. The integration of the element thrust and torque over the propeller radius for all the blades gives the total thrust and torque of the propeller.

Consider the radius r with element dr as shown in Figure 2, the resultant velocity is considered to include an axial velocity V_0 together with a rotational velocity $V_2 = \omega r$ which clearly varies up to the blade tip. These three velocity components are demonstrated in Figure 3. The induced flow input from other sections is negligible. Since the propeller blade will be set at a given geometric pitch angle (θ), the local velocity vector will create a flow angle of attack on the section. The lift and drag of the section can be calculated using standard 2D hydrofoil properties. (Note: Change of reference line from chord to zero lift line.) The lift and drag components normal to and parallel to the propeller disk can be calculated
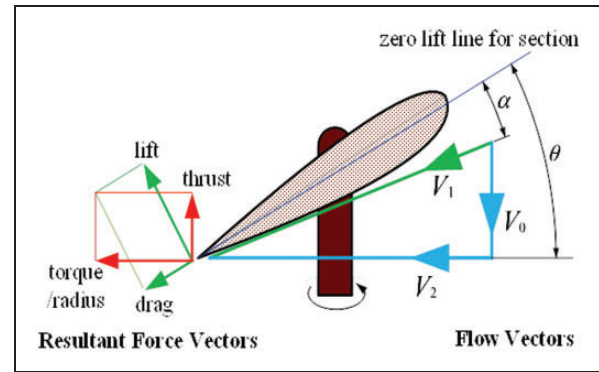
so that the contribution to the thrust and torque of the complete propeller from this single element can be found.

The incident angle is difference between geometric angle and hydrodynamic angle defined as

$$\alpha = \theta - \varphi$$

If the number of propeller blades is Z then for the propeller, the thrust and torque are measured by

$$T = \int \left[\frac{1}{2} \rho Z c V_1^2 (c_1 \cos(\alpha) - c_d \sin(\alpha)) \right] dr \quad (8)$$

$$Q = \int \left[\frac{1}{2} \rho Z c V_1^2 (c_1 \sin(\alpha) - c_d \cos(\alpha)) r \right] dr \quad (9)$$

where ρ is the water density, c is the blade chord so that the lift producing area of the blade element is $c.dr$, c_1 and c_d are respectively the lift and drag coefficients, and r is the blade radius.

The thrust and torque coefficients and the open water efficiency of the propeller are respectively as follows

$$K_T = \frac{T}{\rho n^2 D^4} \quad (10)$$

$$K_q = \frac{Q}{\rho n^2 D^5} \quad (11)$$

$$\eta_o = \frac{K_T}{K_q} \frac{J}{2\pi} \quad (12)$$

where n, D, and J are the rotational speed of the propeller, the diameter of the propeller, and the advance velocity coefficient, respectively. T and Q are also the propeller thrust and torque.

The relations of the advance velocity coefficient and the axial velocity are as follows

$$J = \frac{V_0}{nD} \quad (13)$$

$$V_0 = V(1 - w) \qquad (14)$$

where w is the wake fraction and is related to the block coefficient (C_B)[33] by

$$w = 1.7643\, C_B^2 - 1.4745\, C_B + 0.2574 \qquad (15)$$

The calculated propeller thrust (T_{Cal}) must be equal or more than the total ship resistance. The propeller thrust and the minimum required thrust (T_R) can be calculated as follows

$$T_{Cal} = K_T \rho\, n^2 D^4 \qquad (16)$$

$$T_R = \frac{R_T}{n_p(1 - t_{de})} \qquad (17)$$

$$t_{de} = 0.25w + 0.14 \qquad (18)$$

where R_T is the total resistance of the ship, n_p is the number of the propeller, and t_{de} is the thrust deduction factor as a function of the wake fraction.[34] Then, K_T is used in calculations as follows

$$K_T = AJ^2 \qquad (19)$$

where A is indicated in equation (20)

$$A = \frac{T_R}{\rho \times V_0^2 \times D^2} \qquad (20)$$

The advance coefficient (and thus the propeller r/min) and corresponding propeller efficiency are obtained from the intersection of K_T (equation (19)) and the open water diagram of propeller as illustrated in Figure 4.
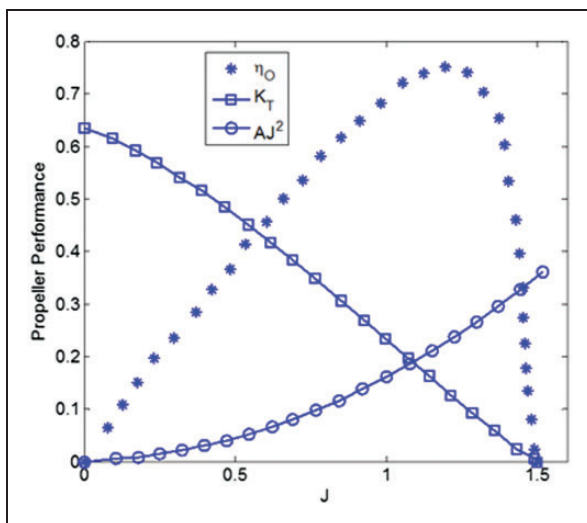

Figure 4. Example of the intersection of AJ^2 and K_T diagrams.

Skew effect

An effective idea for diminishing cavitation, vibratory pressures and shaft forces is to employ extreme skew. It is obvious that when the blades are sufficiently skewed, the sections gradually pass through the crest of the wake thus the oscillating forces are decreased in comparison with a blade whose location of mid-chords is radially straight. On the other hand, high skew angle could also reduce efficiency. The effect of the skew on the propeller efficiency indicates that an approximate formula may be obtained for efficiency in terms of the skew angle.[23]

$$\frac{\eta_{Skew}}{\eta_o} = 0.06687e^{-0.1148\theta_s} + 0.989e^{-0.001029\theta_s} \qquad (21)$$

where θ_s is the skew angle in degrees and η_o is the open water efficiency. According to this equation there is an inverse relationship between the efficiency of skewed propeller and the skew angle.

Cavitation constraint

Burrill's diagram is one of the best known cavitation criteria for conventional marine propellers. This diagram gives the limit value of a thrust loading coefficient τ_c as a function of the cavitation number $\sigma_{0.7R}$. Another best known criterion which may be utilized to obtain the expanded blade area required to avoid cavitation is based on Keller's.[34] It is generally known that cavitation could affect a propeller's performance and need to be considered during the design process. A simple way to reduce the cavitation is to increase the blade area ratio. Here, the Keller criterion is expressed as follows

$$\frac{A_E}{A_{o\,\min}} = \frac{(1.3 + 0.3z)T}{(P_0 - P_V)D^2} + K \qquad (22)$$

where $\frac{A_E}{A_{o\,\min}}$ is the minimum blade area ratio, P_0 and P_V are the static pressure at the centerline of propeller shaft and the vapor pressure and the coefficient K equals to 0.1 for twin propeller, and 0.2 for single propeller.

Propeller strength constraint

Due to the complex shape of propeller blades, the accurate calculation of the stress resulting from the thrust and torque of propeller and the centrifugal force on each blade is extremely difficult. If the blade center of mass locates in radius $\bar{r} = \int_{r_0}^{R} a\, r\, dr / \int_{r_0}^{R} a\, dr$, the centrifugal force is calculated by

$$F_C = m_b \bar{r}(2\pi n)^2 \qquad (23)$$

where m_b is the blade mass from radius r_0 to the blade tip. So the moments due to centrifugal force are

$$M_R = F_c z_c \tag{24}$$

$$M_s = F_c y_c \tag{25}$$

where y_c and z_c are the space between the centroids of the blade and the section. M_R and M_s are the moments due to rake and skew angles, respectively. So the stress (St) in the section is

$$St = \frac{M_{x0}}{I_{x0}/y_0} - \frac{M_{y0}}{I_{y0}/x_0} + \frac{F_C}{a_0} \tag{26}$$

where

$$
\begin{aligned}
M_{x0} &= -(M_T + M_R)\cos\theta - (M_Q - M_S)\sin\theta \\
M_{y0} &= -(M_T + M_R)\sin\theta - (M_Q - M_S)\cos\theta
\end{aligned}
\tag{27}
$$

where θ is the pitch angle, I_{x0} and I_{y0} are respectively the section modulus about the $x0$ and $y0$ (the axes of the centroid of the section) and a_0 is the area of the section. It is obvious that the cantilever beam theory is widely used to estimate the maximum tensile or comparison stress in any blade section. For performing the above-mentioned procedure we first of all create a propeller geometry and then divide the blade sections into 26 stations in chord direction and 11 sections in radial, thereafter we do integrating by Simpson's method for the calculation of the volume, momentum of inertia and area, then compute the moments of thrust and torque and at the last step estimate the stress in blade sections (root, 0.25 R, and 0.3 R). The amount of stress obtained by this technique should be less than the maximum allowable stress of the propeller material.

Specific fuel oil consumption

The SFOC is provided by engine manufacturers as a function of engine load. In order to determine the fraction of engine load, the power requirements must be known. The effective power of the vessel, P_E, relates the vessel resistance and speed by

$$P_E = R_T V \tag{28}$$

The resulting delivered power, P_D, can be calculated using equation (29)

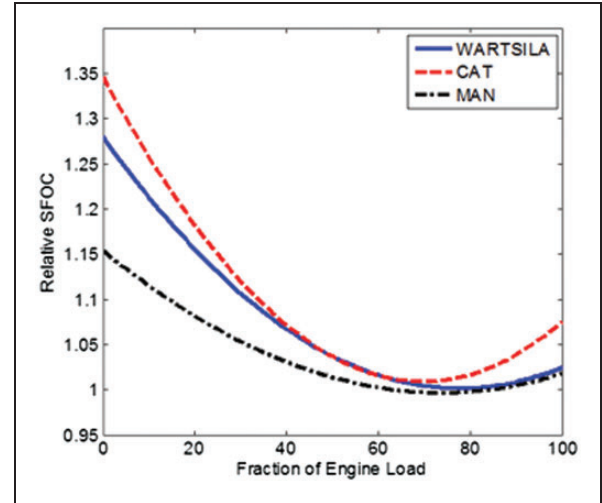$$P_D = \frac{P_E}{QPC} \tag{29}$$

Figure 5. The relative specific fuel oil consumption (SFOC) as a function of percentage of load based on the data of three engine manufacturers: Wartsila, Caterpillar, and MAN.

where QPC is the quasi-propulsive-coefficient given by the product of three efficiencies affecting the hull and propeller

$$QPC = \eta_H \eta_{RR} \eta_o \tag{30}$$

where η_H is the hull efficiency as shown in equation (31), $\eta_{RR} = 1.0$ is the assumed relative rotative efficiency, and η_o is the open water efficiency as calculated in equation (12).

$$\eta_H = \frac{1-t}{1-w} \tag{31}$$

In this work, the losses due to shaft and bearing efficiencies are assumed to be negligible. Once the power is calculated the SFOC at any speed can be found based on the percentage of load. The relative SFOC curves provided by the engine manufacturers Wartsila, MAN, and Caterpillar are presented in Figure 5. The data of Caterpillar[35] and MAN[36] are based on three different SFOC-curves of relatively small four-stroke engines and large two-stroke engines, respectively. Wartsila data for "46f" medium sized engine family is used.[37]

In this study, we have used the regression analysis of the relative SFOC data from Wartsila, CAT, and MAN to fit a quadratic function to each curve and these second order polynomial equations are respectively as follows

$$
\begin{aligned}
SFOC_{Relative-W} &= 0.4613 EL^2 - 0.7168 EL + 1.28 \\
SFOC_{Relative-C} &= 0.7024 EL^2 - 0.97728 EL + 1.35 \\
SFOC_{Relative-M} &= 0.2933 EL^2 - 0.432 EL + 1.1565
\end{aligned}
\tag{32}
$$

Table 1. Base value of specific fuel oil consumption (g/kWh) according to engine age, stroke type, power, and build year.[36]

Build year	2-stroke	4-stroke (>5000 kW)	4-stroke (1000-5000 kW)	4-stroke (<1000 kW)
1970–1983	180–200	190–210	200–230	210–250
1984–2000	170–180	180–195	180–200	200–240
2000-	165–175	175–185	180–200	190–230

where EL is the fraction of engine load. The absolute SFOC is defined as

$$SFOC = SFOC_{Relative} \times SFOC_{base} \qquad (33)$$

The relative SFOC ($SFOC_{Relative}$) can be used for predicting ship emissions. The base value for $SFOC_{base}$ is a constant for each engine and varies according to Table 1.[38]

Lifetime fuel consumption

In order to evaluate the ship performance over its operating life, we use the likelihood of an operating condition such as speed and sea state. By considering the probability density function (PDF) of ship speed the LFC can then be estimated. The type of vessel is the main factor that affects the operational profile; for example, a naval combatant and a merchant vessel may have a highly bimodal and unimodal distribution respectively. The clear advantage of employing a PDF indicating the mission profile of the vessel is to avoid designing a ship that is significantly sub-optimal at off-design speeds. A probability distribution for a container ship has been explained in Temple and Collette[39] and is shown in Figure 6.

After the resulting delivered power (P_D) and specific fuel oil consumption ($SFOC$) are obtained the LFC is weighted by the operational probabilistic density function (P) and integrated over the entire operating range. The integral, shown in equation (34), is multiplied by the life time hours, L_h, in order arrive at the estimated LFC.

$$LFC = \int \{P(V)\, SFOC(V) P_D(V) \mathrm{d}V\, L_h\} \qquad (34)$$

Multi-objective optimization

The general mathematical form of a numerical constrained optimization problem has been represented here. Design variables and constraint conditions are used to characterize the problem. The role of design variables in ship optimization problems is controlling the geometry of the hull during optimization procedure. Constraints are the values by which the design variables are restricted and may be separated in two types, equality and inequality constraints. A function
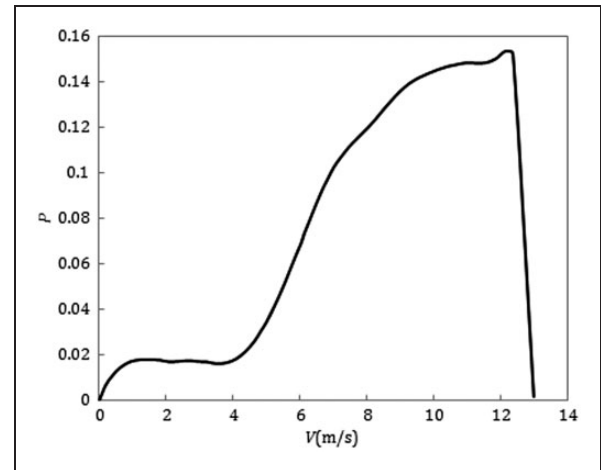
Figure 6. Probabilistic speed profile for a container ship.

being maximized or minimized by users is known as the objective function and the value of this function is a criterion to determine the efficiency of design optimization methodology. If in an optimization problem only one objective function is used the optimization is known as single objective and if two or more objective functions are used the optimization is known as multi objective. The standard formulation of a MOP is mathematically as follows

$$Optimize\ F(X) = [f_1(X), f_2(X), \ldots, f_m(X)]^T$$
$$X \in \mathcal{R}^n$$

Subject to some equality and inequality constraints

$$h_i(X) = 0 \quad i = 1, 2, \ldots, p \qquad (35)$$

$$g_j(X) \leqslant 0 \quad j = 1, 2, \ldots, q \qquad (36)$$

where $f_i(X)$ is the objective function, m is the number of objective function, p is the number of the equality constraints, q is the number of the inequality constraints and $X = (x_1, \ldots, x_n) \in \Im \subseteq \mathbb{C}$ is a solution or individual vector. The set $\mathbb{C} \subseteq \mathbb{R}^n$ defines the search space and the set $\Im \subseteq \mathbb{C}$ defines a feasible search space.

When we have solved the MOP, we will have found a multitude of solutions. Only a small subset of these solutions will be of interest. For a solution to be interesting there must exist a domination relation between

the solution considered and other solutions in the following sense:

We say that a vector U dominates a vector V if U is at least as good as V for all the objectives, and U is strictly better than V for at least one objective.

$$\forall i \in \{1, 2, \ldots, n\}, u_i \leqslant v_i \ \wedge \ \exists j \in \{1, 2, \ldots, n\}, \ u_j \leqslant v_j$$

Solutions which dominate the others but do not dominate themselves are called Pareto set (or nondominated solutions) and their corresponding objective functions are called Pareto front.[40]

Nondominated sorting genetic algorithm-II

NSGA-II is a well-known fast and elitist multi-objective genetic algorithm that is used in this paper. The nondominated sorting method is an important characteristic of NSGA-II. The following are the steps of the NSGA-II:[41]

1. Initialize the population

2. While the termination criterion is not met repeat the following:
   (a) Evaluate each solution in the population by computing objective function values.
   (b) Rank the solutions in the population using nondominated sorting.
   (c) Perform selection using the crowded binary tournament selection operator.
   (d) Perform cross over and mutation (as in conventional GA) to generate the offspring population.
   (e) Combine the parent and child populations.
   (f) Replace the parent population by the best members (selected using nondominated sorting and the crowded comparison operator) of the combined population.
3. Output the first nondominated front of the population

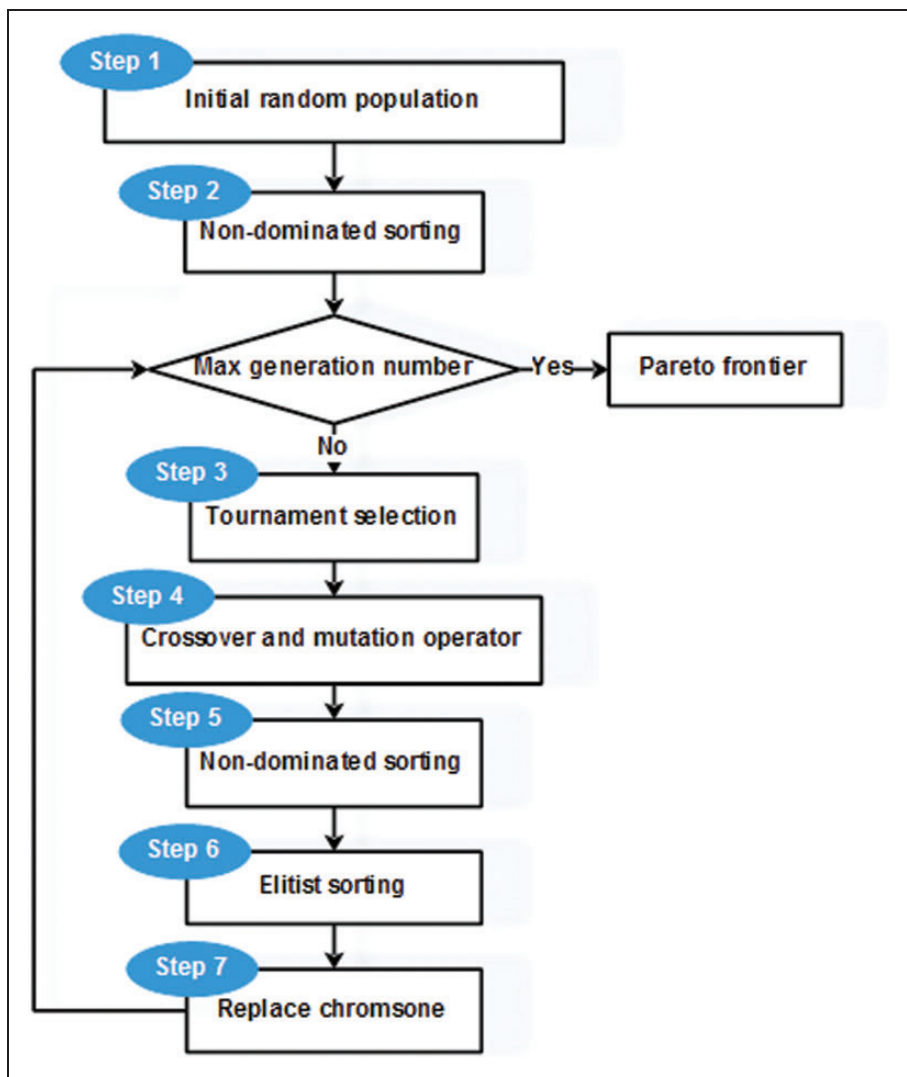A brief description of the algorithm is given in Figure 7.
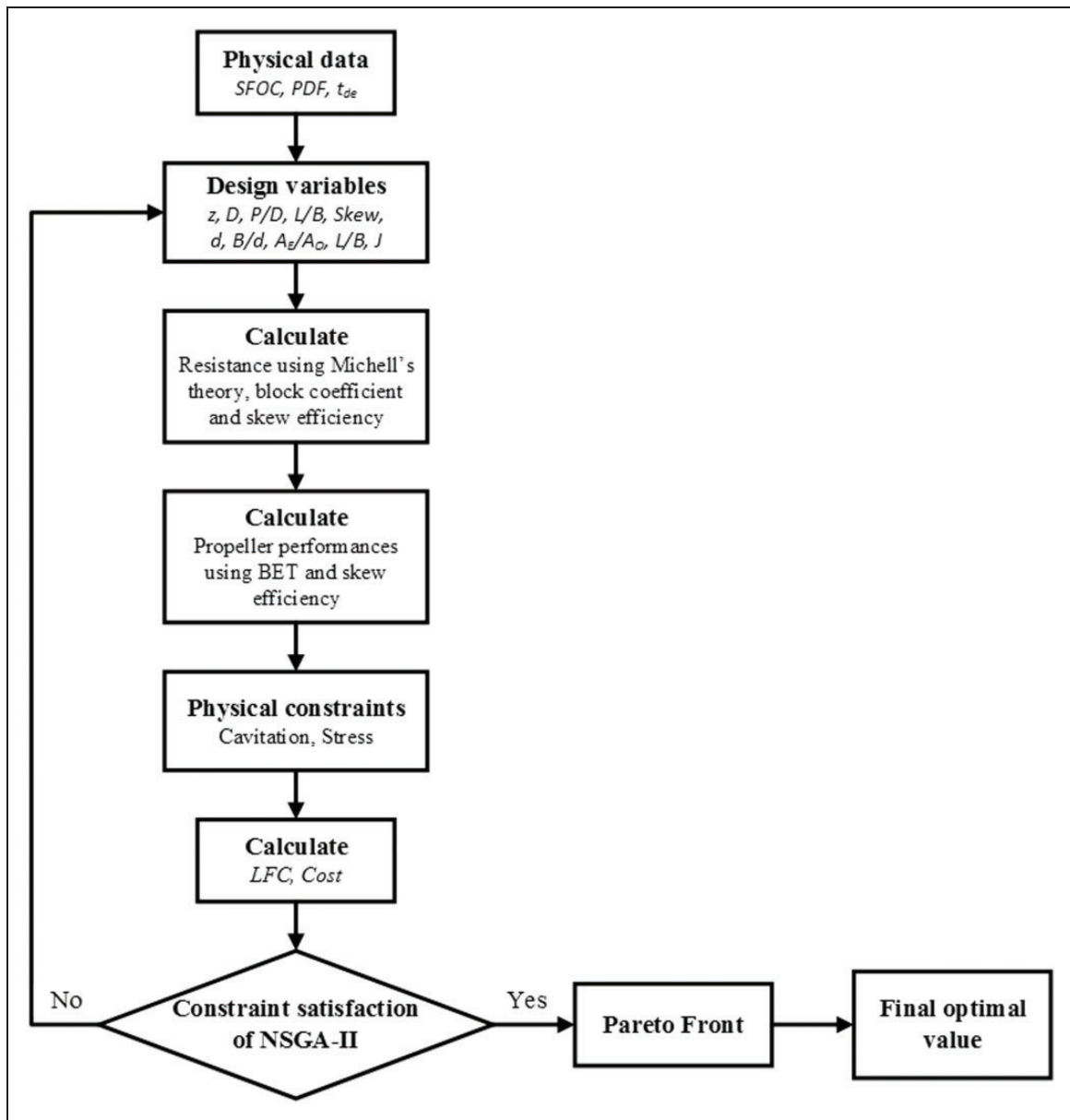

Figure 7. General schematic of the NSGA-II.

Figure 8. Flowchart of the hull–propeller optimization process.

Program implementation

Figure 8 demonstrates how the aforementioned methods and techniques are utilized to optimize the hull–propeller system. First, the initial population is made up of individuals including design variables that are randomly chosen within their limits (the limits come later). By employing the Michell's theory and ITTC-57 correction line formula the total resistance is calculated for each individual. The operating advance coefficient (and hence the required propeller rpm), the propeller performance and skew efficiency at this design advance coefficient are then obtained using BET based on the known values of R_T from previous step and the design variables.

If the physical constraints, the cavitation and propeller stress, are not satisfied the objective functions

are penalized by penalty function. After that to consider the operational lifetime of the vessel in the optimization process the *LFC* and *Cost* functions, two lifetime objective functions used in this work, are computed by taking into account the probabilistic mission profile of the vessel. The *Cost* function is a linear combination of the open water and skew efficiencies, thrust and torque of the lifetime of the propeller as already mentioned. Finally the algorithm is repeated and once the algorithm reaches its maximum generation, the Pareto front is drawn and the final optimal solution is selected by a decision making skill. In this paper, we select the solution that is as close as possible to utopia point as schematically illustrated in Figure 9. This point is called compromise solution and here is denoted as the CS which is chosen for comparison with initial solution (IS) in the latter discussion. To obtaining the compromise solution
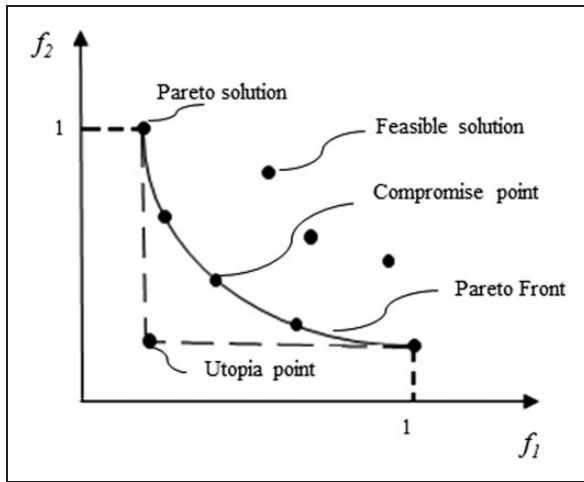
Figure 9. Pareto front and Utopia and Compromise points in MOP.

Table 2. Parameter settings of NSGA-II.

Type of parameter	Value
Max generation	1100
Population size	7
Rate of mutation	30%
Mutation type	Random
Rate of recombination	70%

(CS), the objective functions are normalized first and the distance between each solution on the Pareto front and the utopia point is measured. Eventually the solution having minimum distance is selected as the CS. Before applying the NSGA-II we need to choice appropriate parameter settings. In this study the parameter settings of the algorithm are presented in Table 2. For $m = 2$ and $n = 9$, the standard formulation of the MOP presented in this work is as follows

$$F(X) = [f_1(X), f_2(X)]^T \qquad X \in \mathcal{R}^9 \qquad (37)$$

where

$$f_1(X) \equiv Cost = \sum_{i=1}^{4} w_i * I_i(X)$$

$$f_2(X) \equiv LFC = \int P\,(V)\,SFOC(V)P_D(V)\mathrm{d}V\,L_h \qquad (38)$$

Here, $I_i(X)$ is defined for four parameters as follows

$$I_1(X) = \int P\,(V)\,T(V)\mathrm{d}V$$

Table 3. The performance weights in *Cost* function.

Performance	Thrust ($i = 1$)	Torque ($i = 2$)	Open water efficiency ($i = 3$)	Skew efficiency ($i = 4$)
Weight (w_i)	0.2	0.3	0.2	0.3

Table 4. Limits of the design variables vector.

Design variable	Lower limit	Upper limit
Number of blades, Z	2	7
Skew angle (deg)	10	20
Maximum allowable stress (Pa)	0	39,000
Pitch ratio, P/D	0.5	1.4
Propeller diameter (m)	4.4	10.8
Expanded area ratio, EAR	0.55	1.05
Draft (m)	8.8	12
Breadth-to-draft ratio, B/d	1.2	3.6
Length-to-breadth ratio, L/B	5	8

$$I_2(X) = \int P\,(V)\,Q(V)\mathrm{d}V$$

$$I_3(X) = \int P\,(V)\,\eta_O(V)\mathrm{d}V$$

$$I_4(X) = \int P\,(V)\,\eta_{Skew}(V)\mathrm{d}V \qquad (39)$$

Subject to two constraints of the stress (St) and cavitation

$$g_1(X) \equiv St < 39000$$

$$g_2(X) \equiv \frac{(1.3 + 0.3Z)T}{(P_O - P_V)D^2} + K \leqslant EAR \qquad (40)$$

where the design variables vector is

$$X = \left[L/B,\ B/d, d, EAR, Z, D, P/D, Skew \right] \qquad (41)$$

The weights of thrust, torque, open water efficiency, and skew efficiency of the *Cost* function and the limits of the design variables vector are tabulated in Tables 3 and 4, respectively. Because the torque and skew efficiency do not play a role in obtaining the *LFC* function, the thrust and open water efficiency have greater weights in the *Cost* function.

Results and discussion

The results and analysis of the optimization run using the previously defined objective and constraint functions are presented in this section. Calculations were
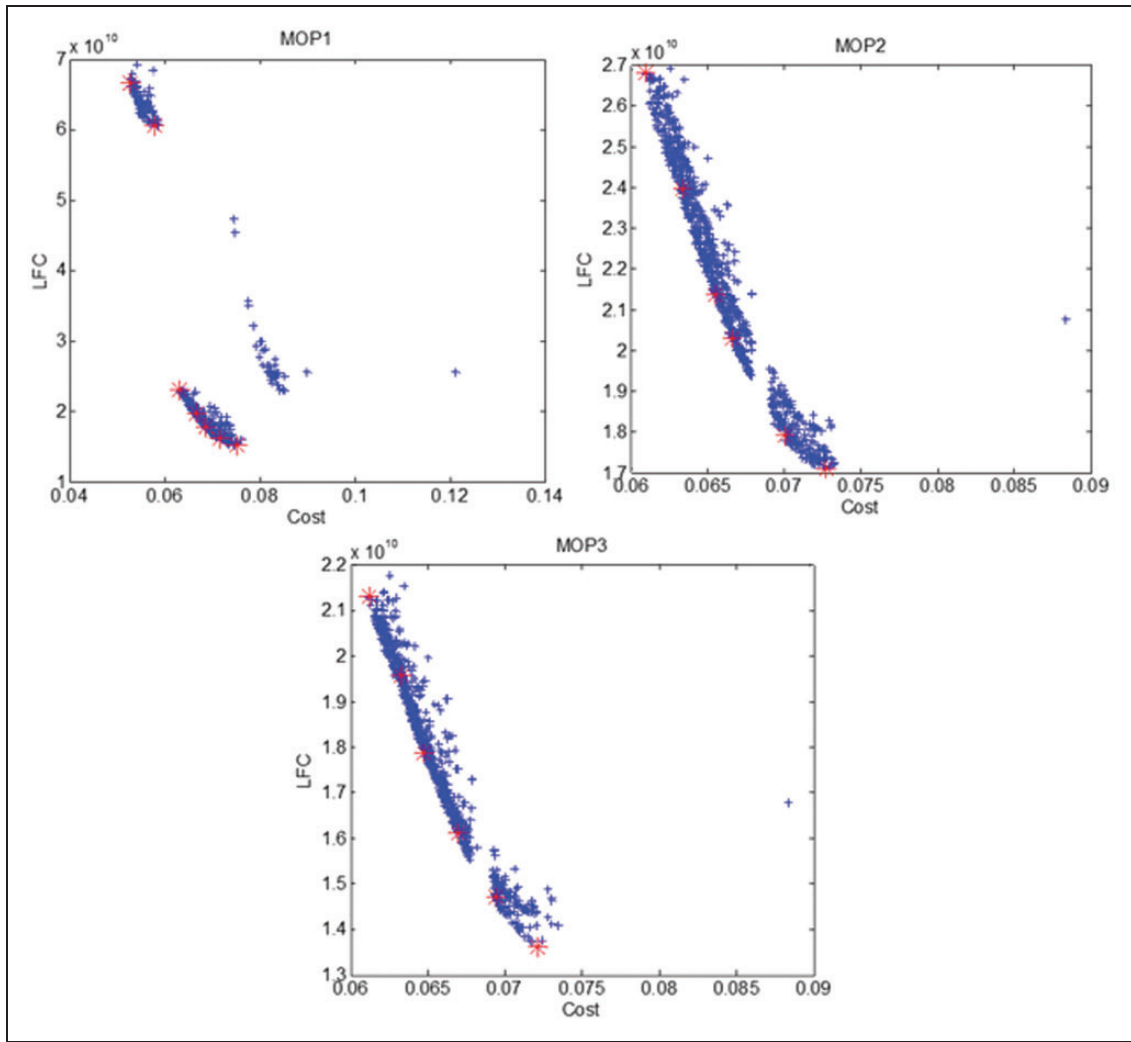
Figure 10. Evolution of the Pareto fronts during optimization for three engine manufacturers.

made on a Windows-based personal computer having 2.4 GHz CPUs. The averaged time for running this program code on each problem was about 9 h.

The NSGA-II was run on the problems based on the SFOC curves of three engine manufacturers (Figure 5): Wartsila (MOP1), Caterpillar (MOP2) and MAN (MOP3), and the Pareto fronts obtained in each generation are illustrated in Figure 10 by blue plus symbols. The red star symbols in the figure specifically depicted in Figure 11 denote that the NSGA-II is able to promote the spreading of the individuals along the Pareto front. Figure 11 reports Pareto optimal fronts for three different MOPs.

The results confirm that there is an apparent conflict between the *LFC* and *Cost* objective functions. In other words increasing in LFC will lead to decreasing in Cost and vice versa.

The CSs of the MOPs

The values of the initial and Pareto optimal solutions of the three MOPs, which have been obtained using
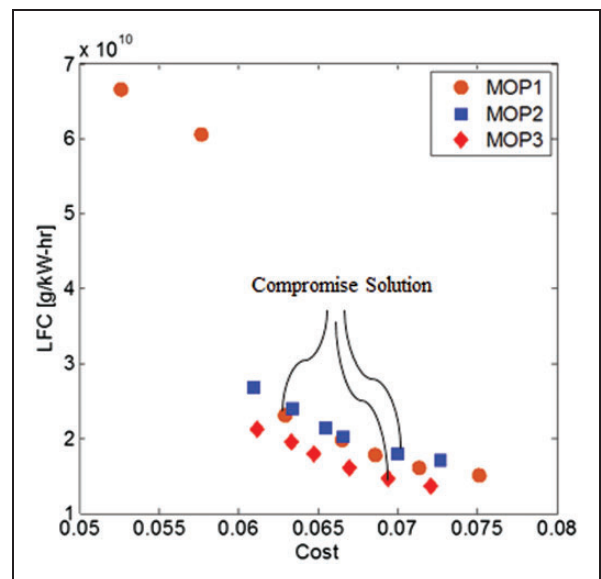

Figure 11. Pareto optimal fronts for different MOPs.

Table 5. The initial and optimal solutions (Pareto front) based on the SFOC curve of Wartsila (MOP1).

Parameter	Initial value	Optimal value 1	Optimal value 2	Optimal value 3	Optimal value 4	Optimal value 5	Optimal value 6	Optimal value 7
L/B	7.44	7.87	7.84	7.87	7.85	7.86	7.87	7.02
B/d	3.5	1.29	2.33	1.29	2.24	2.24	2.09	1.4
d	10.15	8.8	11.82	8.8	11.09	8.86	8.8	9.21
EAR	0.89	0.55	0.55	0.55	0.55	0.55	0.55	0.55
Z	4	3	3	3	3	3	3	3
D	7.21	5.79	4.41	5.79	4.63	4.66	5.79	4.73
P/D	1.14	1.36	0.85	1.36	0.89	0.95	1.36	0.97
$Skew$	18.91	10.19	10.09	10.19	10.12	10.12	10.19	10.15
$LFC*10^{12}$	6.05	0.136	6.35	0.136	3.00	0.639	0.373	0.241
$Cost$	0.073	0.074	0.055	0.074	0.056	0.06	0.063	0.071

Table 6. The initial and optimal solutions (Pareto front) based on the SFOC curve of Caterpillar (MOP2).

Parameter	Initial value	Optimal value 1	Optimal value 2	Optimal value 3	Optimal value 4	Optimal value 5	Optimal value 6	Optimal value 7
L/B	5.2	7.91	7.9	7.91	7.89	5.3	7.9	7.89
B/d	3.06	2.34	1.29	2.34	1.91	2.34	1.36	2.11
d	11.48	12	9.01	12	9.87	12	9.22	11.99
EAR	0.79	0.55	0.55	0.55	0.55	0.55	0.55	0.55
Z	3	3	4	3	4	3	4	3
D	7.07	4.51	5.35	4.51	4.86	4.51	5.35	4.59
P/D	1.15	0.81	1.39	0.81	1.37	0.81	1.17	0.87
$Skew$	13.83	10.26	10.04	10.26	10.1	10.26	10.05	10.25
$LFC*10^{12}$	1.16	2.01	0.0568	2.01	0.223	0.779	0.0856	1.28
$Cost$	0.07	0.055	0.073	0.055	0.061	0.057	0.071	0.056

the NSGA-II, are listed in Tables 5–7. The CSs of the three MOPs in Figure 11 correspond to optimal values 4, 5, and 5 given in Tables 5–7, respectively. The comparison between the IS and CS of the three MOPs is reported in Table 8.

Hull dimensions effect

Regarding to the variation of L/B, B/d, and d, the hull dimensions (L, B, and d) of the CS are increased with respect to those of the IS for MOP1. The length is increased and the beam and draft are reduced for MOP2 and MOP3. From the hydrodynamic point of view it is obvious that the increase of hull length and the reduction of hull beam and draft have a positive effect on the ship's resistance and causes in a relative reduction in LFC. Also an increased B/d ratio results in general in an increase of the range of stability.

Diameter (D) effect

Regarding to the propeller design variables, an increase of propeller diameter leading to an increase

in efficiency and the risk of cavitation, therefore D should be designed and selected in such a way to reduce cavitation and increase efficiency. In general and in the absence of other constraints, the propeller diameter is selected in the range of 60–90% of ship's design draft. The obtained values of D seem to be reasonable values for the practical applications.

Expanded aria ratio (EAR) and number of blades effect

The values of propeller EAR are lowered for all cases except for MOP1 which is approximately remained fixed. The higher the EAR value, the heavier the propeller weight and the more LFC. The results show that the best values of both the objective functions are for a system with 3 to 5 propeller blades, because the other number of the propeller blades reduces the values of one or both of the objective functions.

Pitch ratio (P/D) effect

Increasing the pitch ratio leads to increase in the propeller thrust and torque and, thus, the possibility

Table 7. The initial and optimal solutions (Pareto front) based on the SFOC curve of MAN (MOP3).

Parameter	Initial value	Optimal value 1	Optimal value 2	Optimal value 3	Optimal value 4	Optimal value 5	Optimal value 6	Optimal value 7
L/B	6.58	7.93	6.84	6.84	6.94	7.78	7.81	7.93
B/d	2.88	2.29	1.51	1.51	2.12	2.16	2.16	2.29
d	10.86	11.75	8.85	8.85	9.32	11.46	10.01	11.75
EAR	0.85	0.66	0.62	0.62	0.62	0.65	0.66	0.66
Z	5	5	4	4	4	5	4	5
D	5.95	4.53	5.78	5.78	4.88	4.54	5.08	4.53
P/D	1.06	0.95	1.39	1.39	1.36	1.08	0.96	0.95
Skew	16.6	10.1	10.3	10.3	10.2	10.1	10.3	10.1
$LFC*10^{12}$	1.62	2.56	0.0812	0.0812	0.250	1.45	0.552	2.56
Cost	0.07	0.056	0.071	0.071	0.062	0.057	0.059	0.056

Table 8. Comparison of design variables and objective functions between IS and CS of the three MOPs.

Problem / Parameter	MOP1		MOP2		MOP3	
	IS	CS	IS	CS	IS	CS
L/B	7.44	7.86	5.2	7.89	6.58	6.94
B/d	3.5	2.24	3.06	1.91	2.88	2.12
d	10.15	8.86	11.48	9.87	10.86	9.32
EAR	0.89	0.55	0.79	0.55	0.85	0.62
z	4	3	3	4	5	4
D	7.21	4.66	7.07	4.86	5.95	4.88
P/D	1.14	0.95	1.15	1.37	1.06	1.36
Skew	18.91	10.12	13.83	10.1	16.6	10.2
$LFC*10^{12}$	6.05	0.639	1.16	0.223	1.62	0.250
Cost	0.073	0.06	0.07	0.061	0.07	0.062

IS: initial solution; CS: compromise solution.

occurrence of the cavitation phenomenon enhances. Therefore, this variable should be optimized so that produces enough thrust while preventing the cavitation phenomenon. Considering that all optimal solutions satisfy the cavitation constraint, the resulting pitch ratios can be appropriate values for the selected propellers.

Skew effect

We focused more about the effect of the skew angle in propeller design. The advantages of the skew angle include the elimination of a sudden dynamic load on the blade, conduction of entry flow toward the leading edge, reduction of the fatigue stress while increasing the propeller time endurance (life time). So the selection of optimum value for the skew angle is an important issue. The optimal values of the skew angle for the Pareto optimal solutions change in the small interval, 10.1 to 10.7, which are reasonable values for the B-series propeller.

LFC and Cost

From Tables 5–7 it may be observed that the both objective functions are considerably improved for all optimal solutions of the MOPs. In Table 8 the percentage of the variation of Cost function is about 50% for all MOPs and of LFC is 9, 14, and 12.5 for MOP1, MOP2, and MOP3, respectively. It shows that the LFC of the engine made in CAT (MOP2) is lower in comparison with the other ones.

Propeller performance

The open water performance of the ISs and CSs for the three MOPs is depicted in Figure 12. For the MOP1, the optimum efficiency of the IS and CS is respectively occurred at about 0.75 and 1.08 of *J*, the MOP2 at 0.95 and 1.17, the MOP3 at 0.95 and 1.06. The propeller performance of each of the MOPs at its maximum efficiency is presented in Table 9. It may be observed that the maximum efficiency of
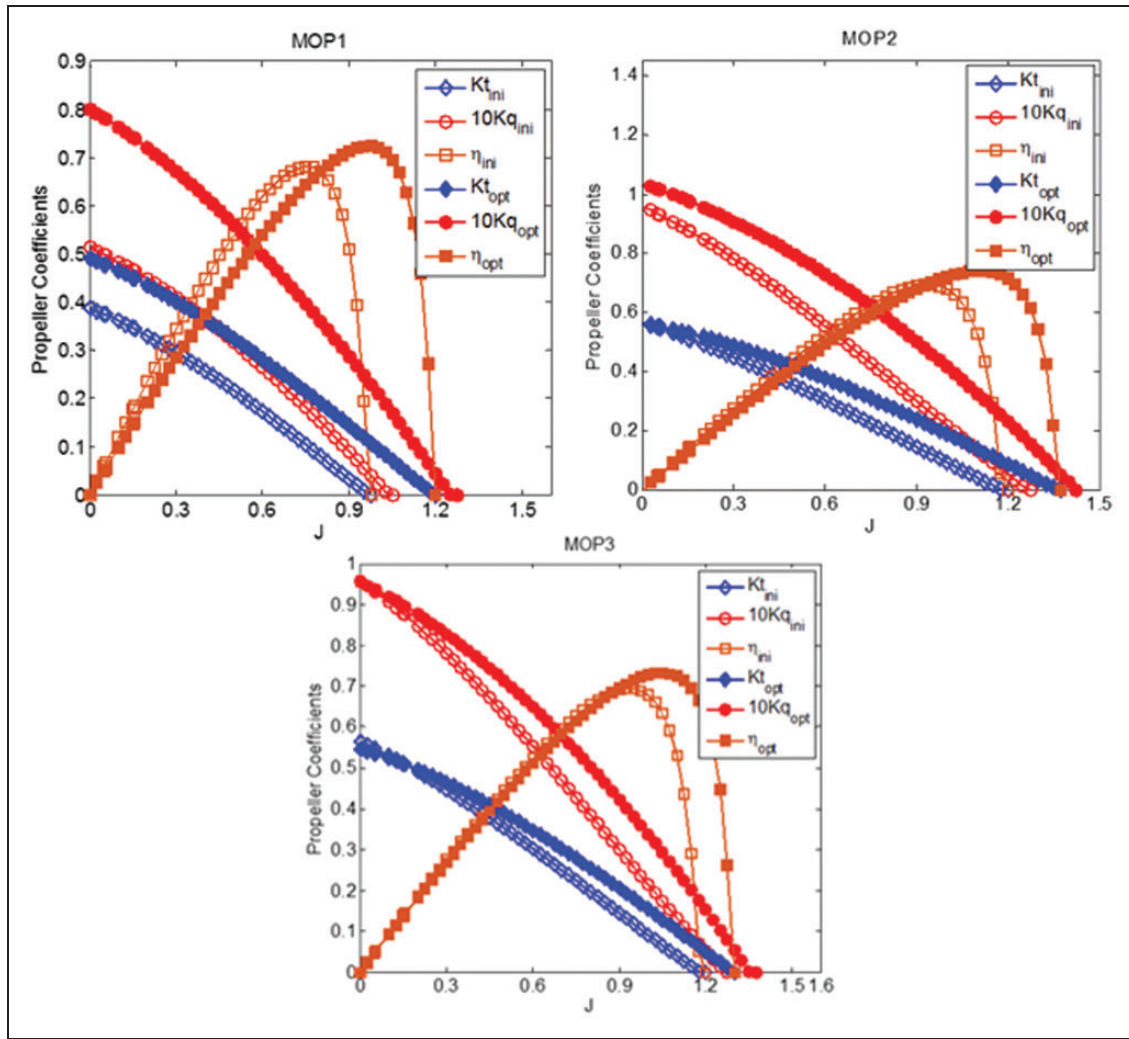
Figure 12. The open water performance of the ISs and CSs of three MOPs.

Table 9. Propeller performance of the MOPs at its maximum efficiency.

Parameter	Problem	MOP1		MOP2		MOP3	
		IS	CS	IS	CS	IS	CS
J		0.95	0.80	0.95	1.20	0.90	1.20
η		0.69	0.71	0.68	0.77	0.70	0.76
K_T		0.13	0.10	0.10	0.13	0.11	0.12
$10K_q$		0.26	0.19	0.25	0.33	0.23	0.3

IS: initial solution; CS: compromise solution.

all the CSs is higher than that of ISs. The thrust coefficient of the CSs is higher than that of ISs for the MOP1 and MOP3. The trend of the torque coefficients is increased for all cases. Higher efficiency of the CSs is equal to 0.75 at $J = 1.17$ for the MOP2.

Resistance and thrust

As a general rule, decrease of ship resistance and propeller torque and increase of propeller thrust

cause in reduction of LFC. Figures 13–15 demonstrate the comparison of the total resistance and thrust of the IS and CS for the three MOPs in terms of the ship speed. As the ship speed increases, the total resistance and propeller thrust increases and decreases respectively. It can be seen that the total resistance of CSs are relatively lower than that of ISs at all speed range except for at a small range for MOP1. Also the propeller thrust of the solutions have a similar trend, so that except for MOP1 the thrust of CSs is higher compared to that of ISs up to the speed of about 10 m/s and after that this relationship is reversed.

Torque

The propeller torque variation of the IS and CS of the three MOPs at different speeds is shown in Figure 16. Although the propeller thrust of CS is lower than that of IS for MOP1, it can be seen from the figure that the propeller torque is significantly reduced compared to the initial one with increasing the ship speed. An opposite trend occurs for the MOP2 and MOP3.
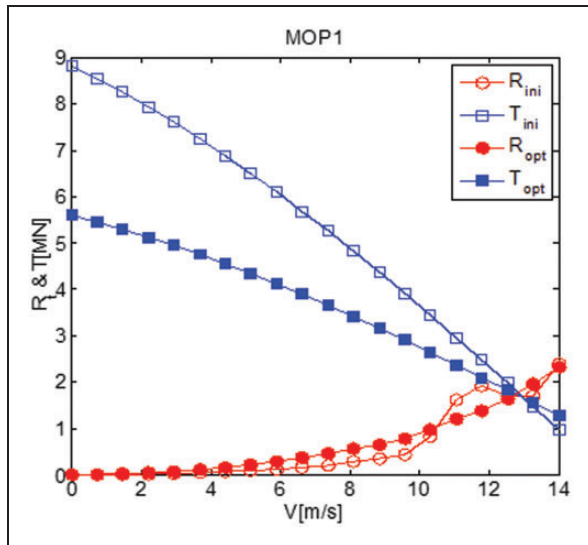
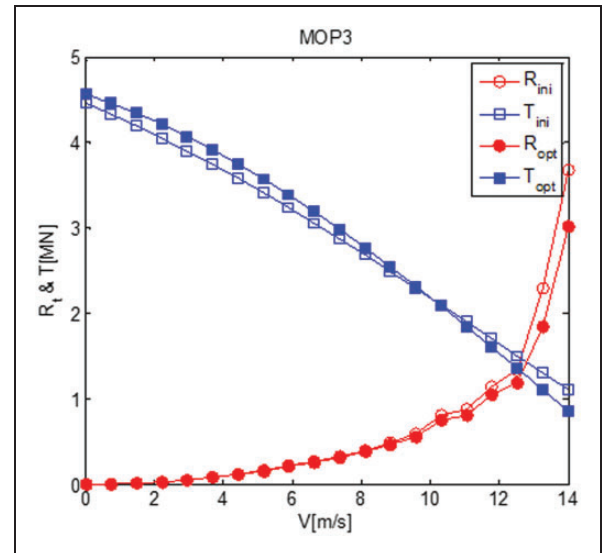**Figure 13.** Hull resistance and propeller thrust of the IS and CS for MOP1.

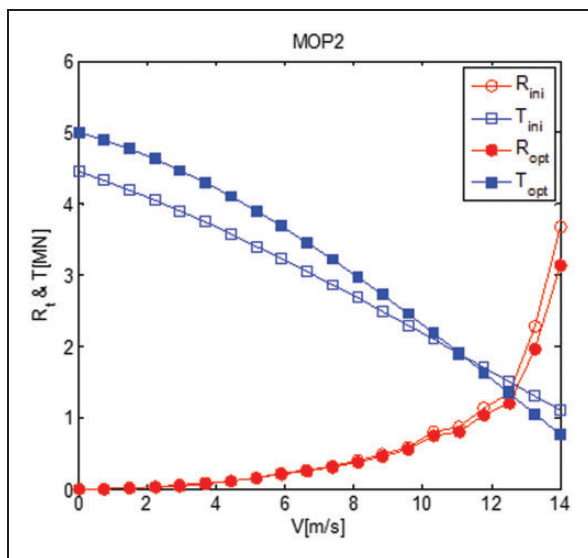**Figure 15.** Hull resistance and propeller thrust of the IS and CS for MOP3.

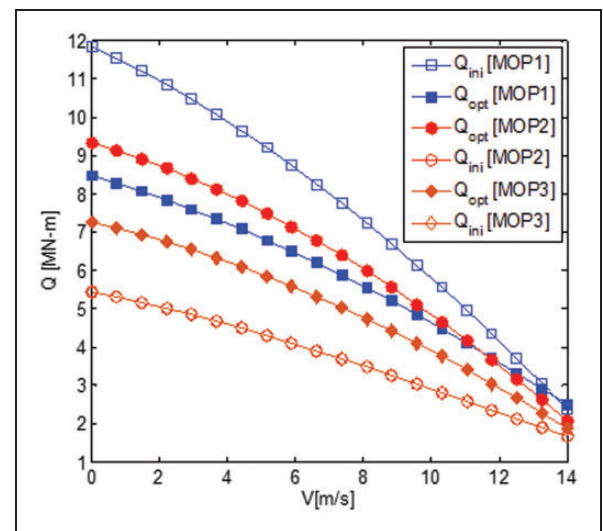**Figure 14.** Hull resistance and propeller thrust of the IS and CS for MOP2.

Figure 16. Propeller torque of the IS and CS for the three MOPs.

Ship design speed

Design speed is found from the intersection point of resistance and thrust force curves. Overcoming the resistance hump is controlled at the same time. By considering Figures 13–15 we found that the design speed of all three MOPs is about $V = 12.7\,\text{m/s}$ which is approximately equal to design speed of the probabilistic speed profile of vessel, $V = 12.35$, (Figure 6) assumed initially. In order to avoid consuming fuel much more we expect that the design point be located below the first hump and in hollow range of resistance curve. As can be seen in the figures all the six

intersection points are located in this range of the resistance curve.

The comparison of the main characteristics of the ISs and CSs of the hull–propeller system for the MOPs at their design speed is reported in Table 10. As can be observed the variation of all main characteristics for MOP1 is small, that is to say the IS and CS are near to each other. On the contrary that is considerable for the other two MOPs. The open water efficiency, skew efficiency, and propeller torque of CSs are increased and the hull resistance and propeller thrust are decreased compared to those of ISs at their design speed.

It is worth noting here that the variation amount of all parameters have been such that both the objective

Table 10. Variation percent of the main characteristics of the hull–propeller system for all the MOPs at the design speed.

Problem	characteristic	η_{Skew}	η_o	Q	$T_{required}$	R_T
MOP1	IS	0.662	0.677	447.81	309.34	249.75
	CS	0.695	0.696	121.21	149.70	125.47
	Variation percent	5	3	72	52	50
MOP2	IS	0.665	0.673	386.36	261.23	213.49
	CS	0.726	0.726	169.74	151.75	128.04
	Variation percent	9.2	7.3	50	42	40
MOP3	IS	0.674	0.686	282.34	250.07	205.94
	CS	0.726	0.726	159.87	142.19	119.43
	Variation percent	7	6	43	43	42

functions are significantly improved. This is approved by comparing the ISs and CSs in Table 8.

Conclusions

This paper has outlined a systematic probabilistic design methodology for simultaneously optimizing the shape of a ship hull–propeller system based on the SFOC curves of the three engine manufacturers, Wartsila, CAT, and MAN as three MOPs. Based on the numerical results, the following conclusions can be drawn:

1. The results were demonstrated that NSGA-II, which was founded Pareto front solutions with good diversity and convergence, is an efficient algorithm to solve the multi-objective optimization problems such as the design problem of the ship hull–propeller. Both the objective functions, LFC and Cost, during the optimization process were improved.
2. Comparison of the CSs for the three MOPs showed that highest efficiency was obtained, 0.75, at $J=1.17$ for the MOP2 (means Caterpillar engine). The efficiency of the CSs at the design speed is 0.695, 0.734, and 0.719 for MOP1, MOP2, and MOP3, respectively.
3. The total resistance and the maximum open water efficiency of all the CSs except for MOP1 at their design speed are improved compared to the ISs. Although the efficiency and thrust were increased for MOP1 at the design speed, the hull resistance was also increased.
4. The propeller torque was significantly reduced compared to the initial one almost at all speed range for the MOP2 and MOP3. Although the propeller torque of the CS was lower than that of the IS for the MOP1, the propeller thrust was also significantly decreased compared to the initial one up to $V=13$ m/s.
5. The intersection point of the resistance and thrust curves (design speed point) of the CSs for all MOPs was obtained approximately near to the assumed design speed in the probabilistic mission profile of the vessel ($V=12.35$) and was located in

the hollow range of the resistance curves as it was expected.

It is our future plan to apply CFD/BEM methods for calculating the hydrodynamics performance of the ship hull and propeller. However, present method for the calculations of the ship and propeller performance is a less time consuming, relatively cost effective and accurate tool.

References

1. Kim J-H, Kim J-H, Yoon J-Y, et al. Application of multi-objective optimization techniques to improve the aerodynamic performance of a tunnel ventilation jet fan. *Proc IMechE, Part C: J Mechanical Engineering Science* 2015; 229: 91–105.
2. Wang W, Wang W, Dong W, et al. Dimensional optimization of a minimally invasive surgical robot system based on NSGA-II algorithm. *Adv Mech Eng* 2015; 7.
3. Sundararaman K, Padmanaban K and Sabareeswaran M. Optimization of machining fixture layout using integrated response surface methodology and evolutionary techniques. *Proc IMechE, Part C: J Mechanical Engineering Science* 2015; DOI: 0954406215592920.
4. Lucas K and Roosen P. *Emergence, analysis and evolution of structures: Concepts and strategies across disciplines.* New York: Springer, 2009.
5. Day AH and Doctors LJ. Resistance optimization of displacement vessels on the basis of principal parameters. *J Ship Res* 1997; 41: 249–259.
6. Dejhalla R, Mrša Z and Vuković S. A genetic algorithm approach to the problem of minimum ship wave resistance. *Marine Technol* 2002; 39: 187–195.
7. Zaraphonitis G, Papanikolaou A and Mourkoyiannis D. Hull form optimization of high speed vessels with respect to wash and powering. *Proc IMDC* 2003; 3: 43–54.

8. Grigoropoulos G, Harries S, Damala D, et al. Seakeeping assessment for high-speed monohulls—A comparative study. In: *8th International marine design conference*, Athens, Greece, 2003.

9. Grigoropoulos GJ and Chalkias DS. Hull-form optimization in calm and rough water. *Comput-Aid Des* 2010; 42: 977–984.

10. Kim H and Yang C. Hydrodynamic optimization of multihull ships. In: *Proceedings of the FAST-11th international conference on fast sea transportation*, Hawaii, USA, 2011.

11. Zakerdoost H, Ghassemi H and Ghiasi M. Ship hull form optimization by evolutionary algorithm in order to diminish the drag. *J Marine Sci Appl* 2013; 12: 170–179.

12. Gaggero S and Brizzolara S. An integrated tool for concept and final design of optimum swat-hull forms. In: *Proceedings of NAV 2006 - international conference on ship and shipping research*, Genova, Italy, 2006.

13. Huang F, Wang L and Yang C. A new improved artificial bee colony algorithm for ship hull form optimization. *Eng Optim*. .

14. Lee Y-J and Lin C-C. Optimized design of composite propeller. *Mech Adv Mater Struct* 2004; 11: 17–30.

15. Cho J and Lee S-C. Propeller blade shape optimization for efficiency improvement. *Comput Fluid* 1998; 27: 407–419.

16. Pluciński MM, Young YL and Liu Z. Optimization of a self-twisting composite marine propeller using genetic algorithms. In: *16th International conference on composite materials*, Kyoto, Japan, 2007.

17. Burger C. Propeller performance analysis and multidisciplinary optimization using a genetic algorithm. ProQuest, 2007.

18. Chen J-H and Shih Y-S. Basic design of a series propeller with vibration consideration by genetic algorithm. *J Marine Sci Technol* 2007; 12: 119–129.

19. Kuiper G. New developments and propeller design. *J Hydrodyn Ser B* 2010; 22: 7–16.

20. Gaafary M, El-Kilani H and Moustafa M. Optimum design of B-series marine propellers. *Alexandria Eng J* 2011; 50: 13–18.

21. Xie G. Optimal preliminary propeller design based on multi-objective optimization approach. *Procedia Eng* 2011; 16: 278–283.

22. Mirjalili S, Lewis A and Mirjalili SAM*Multi-objective optimisation of marine propellersProcedia Comput Sci* 2015; 51: 2247–2256.

23. Kamarlouei M, Ghassemi H, Aslansefat K, et al. Multi-objective evolutionary optimization technique applied to propeller design. *Acta Polytech Hung* 2014; 11.

24. Benini E. Multiobjective design optimization of B-screw series propellers using evolutionary algorithms. *Marine Technol* 2003; 40: 229–238.

25. Greeley DS and Kerwin JE. Numerical methods for propeller design and analysis in steady flow. *Trans-Soc Naval Archit Marine Engrs* 1982; 90: 415–453.

26. Karim MM and Ikehata M. A genetic algorithm (GA)-based optimization technique for the design of marine propeller. In: *Proceedings of the propeller/shafting symposium*, Virginia Beach, USA, 2000.

27. Suen JB and Kouh JS. Genetic algorithms for optimal series propeller design. In: *The third international conference on marine technology*, Poland, 1999, pp.237–246.

28. Motley MR, Nelson M and Young YL. Integrated probabilistic design of marine propulsors to minimize lifetime fuel consumption. *Ocean Eng* 2012; 45: 1–8.

29. Nelson M, Temple D, Hwang J, et al. Simultaneous optimization of propeller–hull systems to minimize lifetime fuel consumption. *Appl Ocean Res* 2013; 43: 46–52.

30. Kelangath S, Das PK, Quigley J, et al. Risk analysis of damaged ships–a data-driven Bayesian approach. *Ships Offshore Struct* 2012; 7: 333–347.

31. Davis PJ and Rabinowitz P. *Methods of numerical integration*. Courier Corporation, 2007.

32. Tuck E, Scullen D and Lazauskas L. Wave patterns and minimum wave resistance for high-speed vessels. In: *24th Symposium on naval hydrodynamics*, Fukuoka, Japan, 2002.

33. van Manen J and van Oossanen P. Propulsion. In: *Principles of naval architecture*. Society of Naval Architects and Marine Engineers, 1988.

34. Ghose J and Gokarn R. *Basic ship propulsion*. New Delhi: Allied Publishers, 2004.

35. Caterpillar Inc. *Caterpillar 3208 Marine engine specification sheet*. Peoria, IL: Caterpillar Inc, 2010.

36. Man Diesel and Turbo, MAN B&W: 6S90ME-C7 Project guide, electronically controlled two-stroked engines, MAN Diesel. 5 ed. Teglholmsgade 41, DK-2450 Copenhagen, Denmark. 2009.

37. Wartsila 46 F Project guide, http://www.wartsila.com/en/engines/medium-speed-engines/Wartsila46F (2013, accessed 4 August 2015).

38. Buhaug Ø, Corbett JJ, Endresen Ø, et al. *Second IMO GHG study 2009*. London: International Maritime Organization (IMO), 2009.

39. Temple D and Collette M. Multi-objective hull form optimization to compare build cost and lifetime fuel consumption. In: *International marine design conference*, IMDC, Glasgow, 2012.

40. Collette Y and Siarry P. *Multiobjective optimization: Principles and case studies*. New York: Springer Science & Business Media, 2013.

41. Deb K, Pratap A, Agarwal S, et al. A fast and elitist multiobjective genetic algorithm: NSGA-II. *IEEE Trans Evolut Comput* 2002; 6: 182–197.

Appendix

Notation

a_0	root section area (m^2)
A_E	propeller expanded area (m^2)
A_O	propeller disk area (m^2)
c_l	lift coefficient
c_d	drag coefficient
C	chord (m)
C/D	chord ratio
C_f	frictional resistance
C_v	viscous resistance
C_w	wave making resistance
D	propeller diameter (m)
EAR	expanded area ratio
F_C	centrifugal force (kN)
I_{x0}	section modulus against x-axis (m^4)
I_{y0}	section modulus against y-axis (m^4)

J	advance ratio
k	form factor
K_t	thrust coefficient
K_q	torque coefficient
L	lift force
L_h	life time (h)
LFC	lifetime consumption (kg)
M_T	thrust moment (kN.m)
M_Q	torque moment (kN.m)
M_R	moment due to rake angle (kN.m)
M_S	moment due to skew angle (kN.m)
n	propeller rotational speed (r/s)
P	probabilistic density function
P/D	pitch ratio
P_D	delivered power
Q	torque force (kN)
$\bar{r}$	root to center of mass of the blade (m)
R_T	total resistance (kN)
Rn	Reynolds number
$SFOC$	specific fuel oil consumption (kg/kW-h)

S_c	maximum allowable stress of the propeller material (MPa)
t_{de}	thrust deduction factor
T	thrust force (kN)
T_R	required thrust (kN)
V_A	advance speed (m/s)
V_S	ship speed (V_R) (m/s)
V_0	axial induced velocity (m/s)
V_1	incident velocity (m/s)
V_2	rotational velocity (m/s)
w	wake factor
z	number of propeller blades
α	angle of attack (deg)
η_o	open water efficiency
η_{skew}	efficiency affected by skew
ω	section rotational speed (rad/s)
φ	hydrodynamic pitch angle (deg)
ρ	water density (kg/m^3)
θ	geometrical pitch angle (deg)
θ_s	skew angle (deg)